ACS OMEGA

http://pubs.acs.org/journal/acsodf

Article

Accurate Concentration Measurement Model of Multicomponent Mixed Gases during a Mine Disaster Period

Feng Li, Chenchen Wang,* Yue Zhang, Xiaoxuan He, Chenyu Zhang, and Fangfei Sha

Cite This: *ACS Omega* 2022, 7, 25443−25457

Read Online

ACCESS | Metrics & More | Article Recommendations

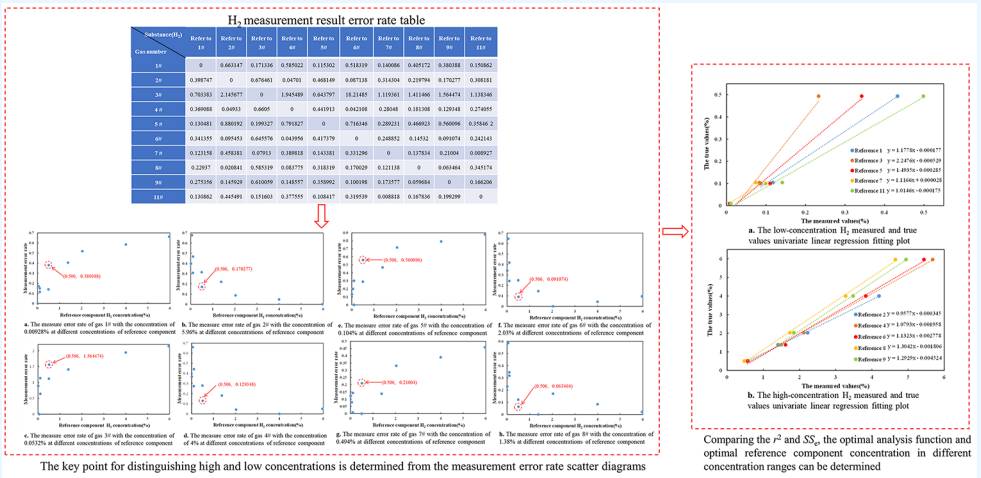

ABSTRACT: A variety of gaseous products are formed when mine fires and coal and gas outbursts occur in mines. On the one hand, these gas products affect the normal production of mines and the occupational health of miners; on the other hand, the gaseous products can also provide much important information to prevent mine disasters. Thus, the rapid and accurate determination of the component content of multicomponent mixed gases is of great significance. However, the distortion of gas chromatography measurement results, which deviate from the true values, has a serious impact on gas composition determination in mines. To reduce the influence of distortion, an Agilent 490 portable gas chromatograph is used to measure the component content of 11 groups of standard multicomponent mixed gases. It is found that the error rate of the measured result is highly related to the concentration of the selected reference component and the component to be measured. Besides, the key point of each gas concentration is determined according to the scatter diagram of the error rate. Each gas is divided into a high and a low concentration group by the key points, and each gas is selected as the reference component to measure the corresponding component concentration in other gases with multiple-point external standards. Researchers have used the least-squares method to fit univariate linear regression analysis between the measured values and true values of mixed gases. Then, the optimal analysis function and the optimal reference component concentration of each gas can be determined by comparing the regression analysis parameters. Finally, it is found that the error rate of measured values corrected by the optimal analysis function is significantly reduced. It is proved that this method can effectively alleviate the measurement results' distortion, which solves the problem of gas composition determination in underground areas.

1. INTRODUCTION

Coal is the most abundant fossil resource on the earth. The issue of safety in mining not only affects the normal production of coal mines but also seriously restricts the development of major coal-producing countries such as China, Poland, the United States, Australia, and so on.[1−6] In mine disasters, mine fires, and coal and gas outbursts, fire damp explosion often occurs in mines, which not only causes casualties and losses of property but also leads to serious social problems.[7,8] Mine fires are mostly caused by coal spontaneous combustion (CSC).[9] CSC is caused by coal oxidation, and the oxidation process is supported by the ability of coal to absorb oxygen, with the simultaneous release of heat.[10]

Received: April 17, 2022
Accepted: July 4, 2022
Published: July 15, 2022

If the heat production rate from the oxidation reaction exceeds the rate of cooling by ventilation or the environment, the temperature will continue to rise. When coal exceeds its critical temperature, it will lead to CSC left in active or sealed longwall goaf.[11−13] During the oxidation process, unstable functional groups, bridge bonds, and radicals are separated from the coal macromolecular structure to form many gaseous products (such as CO, H_2, CO_2, CH_4, C_2H_6, C_2H_4, C_2H_2, and C_3H_8).[14,15] These gaseous products reveal important information on CSC; CO is the first gas generated in these gases, which has a clear corresponding relationship with the coal oxidation temperature.[16,17] Therefore, CO is used as an index gas for predicting CSC in many countries.[4] Xu explored the reaction mechanism of free radicals and functional groups during low-temperature oxidation of coal and the law of active groups producing CO.[18] Jiang analyzed the mechanism of the effect of gas atmosphere conversion on the radical reaction and CO generation rate.[19] Many scholars used other gaseous products (CO_2, C_2H_4, C_2H_6, C_3H_8, etc.) as single-index gases to determine the development state of CSC.[20−22] Although it is more convenient to calculate with single-index gases, this method is influenced by fresh air. Thus, composite index gases have been proposed.[23,24] Hu used composite index gases to analyze drained gas in the upper tunnel, which provides an assessment of CSC in gob.[25] Miao introduced higher-molecular-weight gases to address the blank prediction interval of conventional composite index gases when predicting CSC.[26] Kuchta's research pointed out that if fire cannot be extinguished within 2 h, the fire area should be closed immediately. The flow decrease in the closed fire zone, which is prone to gas accumulation, can lead to gas explosion and even secondary disaster.[27] The US Bureau of Mines studied the variation law of indicator gases in closed fire zones and proposed the explosion triangle method to calculate the explosion risk of combustible gases.[28] Zhou determined the explosion area triangle of the methane explosion limit and the oxygen volume fraction by studying the temperature, pressure, combustible gas, and inert gas concentration in a closed fire zone.[29] Zhou proposed a multiparameter judgment method and related the safety factor model for unsealing the fire area using the BP neural network according to the variation characteristics of index gases.[30] These research results have proved that accurate determination of the component content of multicomponent mixed gases is valuable for understanding the process of fire extinguishment and guiding the fire area unsealing in a closed fire zone.

In addition, an abundance of toxic gases is produced when coal and gas outbursts as well as fire damp explosions occur in mines. These toxic gases not only can cause casualties (such as CO directly inhibits intracellular respiration and causes severe hypoxia in human tissue cells, resulting in damage to the central nervous system and cardiovascular system if miners are exposed to an environment with a high concentration of CO for a long time[10]) but also can move to other tunnels to induce secondary disaster (such as fire damp explosion and gas suffocation).[31] Scholars have studied the distribution of gas concentration after mine gas accidents. Liu divided the propagation of poisonous gases after a fire damp explosion into three stages and established a calculation model for the propagation of poisonous gases in a tunnel.[32] Jia improved the Gaussian puff model according to the actual situation of poisonous gas diffusion and obtained the law of poisonous gas diffusion suitable for fire damp explosion.[33,34] The concentration distribution of these toxic gases not only affects the safety of site miners but also has an important influence on rescue work. According to the "Coal Mine Safety Regulations", after a disaster accident occurs in a mine, mine rescue teams must first be organized to conduct reconnaissance of the disaster area.[34] Due to the complex safety situation of coal mines in China, it is necessary to constantly strengthen the mine rescue teams. There have been 463 full-time coal mine rescue teams, including more than 30 000 commanders and fighters.[35] A large number of rescuers also sacrificed their lives because of the limitation of monitoring technology and equipment. Since 1960, there have been more than 280 accidents in emergency rescue work, and nearly 600 mine emergency rescue fighters have died in mine accidents. Among the casualties, explosion accidents accounted for 46%, poisoning accidents accounted for 33.9%, and suffocation accidents accounted for 10.5%.[36] The main reason for these rescue casualties is the unclear understanding of the concentration of multicomponent mixed gases. It shows that the accurate determination of multicomponent mixed gases plays a vital role in emergency rescue work after gas disasters in mines.

To address the problems caused by unknown gaseous products' concentration, the requirements for quantitative analysis technology have been continuously developed. Quantitative analysis can be divided into chemical analysis and instrumental analysis to determine the amount of multicomponent mixed gases.[37] Chemical analysis is complicated and susceptible to the interference and influence of system random error.[38] Instrumental analysis indirectly reflects the concentration of a substance by the physical properties, such as conductivity, electrode potential, light absorption or emission, mass-to-charge abundance, and fluorescence.[39] Thus, gas detectors can be divided into flame ionization, electron capture, photoionization detector, Fourier-transform infrared spectrometry, X-ray fluorescence spectrometry, mass spectrometry, gas chromatography (GC), and so on according to the different physical properties.[40−42] However, most of these instruments are single-parameter detection equipment, where the detection object is a single gas. Thus, these instruments are insufficient to deal with multicomponent mixed gases.[43] In contrast, GC has the advantages of being able to simultaneously detect multiple gases, having a high separation efficiency for complex mixed substances, and possessing a fast processing speed, simple operation, high quality, and low price. However, when GC is used to detect mixed gases, it leads to loss of target compounds and cross-contamination, affecting the results.[42] According to the GC measurement results of the Xuandong and Liuguantun coal mine in 2006, as shown in Table 1, it was found that the distortion of GC measurement results, which is the sum of component concentrations, severely deviated from 100%. Combined with the above, measuring the mixed-gas concentration accurately plays an important role in preventing CSC and coal and gas outbursts, and hence the distortion of GC measurement results leads to serious trouble in fire extinguishment, the fire area unsealing in a closed fire zone, and emergency rescue work in coal mines.[44] The reason for distortion is that GC cannot make an accurate qualitative judgment on a general unknown system. It can only make more accurate qualitative judgments for systems for which we have prior information on their outline.[45] Thus, calibration is essential to measure the response generated from a sample composed of a known amount of analyte prior to determination of the unknown. At present, there are several types of quantitative methods commonly used, including area percent, single-point external standard, multiple-

https://doi.org/10.1021/acsomega.2c02391
ACS Omega 2022, 7, 25443−25457

Table 1. Measurement Results of Fire Gas Concentration in Xuandong and Liuguantun Coal Mines in 2006

gas number	Xuandong coal mine 1#	Xuandong coal mine 2#	Liuguantun coal mine 3#	Liuguantun coal mine 4#
gas composition		concentrations (%)		
He	0.0006	0.0004	0.0012	0.0007
H_2	0.7857	0.7715	2.0708	1.1803
O_2	11.7948	10.3149	11.6356	14.6132
N_2	84.9099	84.4297	68.3043	71.8538
CH_4	3.5739	5.8736	0.4904	0.2517
CO	0.3947	0.4179	2.165553	1.15708
CO_2	5.5677	6.4891	5.7062	3.5089
C_2H_4	0.0167	0.0274	0.032399	0.016296
C_2H_6	0.2482	0.3147	0.038314	0.019584
C_2H_2	0.0205	0.0023	0	0
sum of component concentrations	107.31	108.64	90.44	92.6

point external standard, single-point internal standard, multiple-point internal standard, and standard addition methods.[46] Due to the range of concentrations or amounts which over the change of the unknown, leading to unclear major, minor, trace, and ultratrace components.[47] Thus, the multiple-point standard is overwhelmingly preferred. To compare the accuracy of multipoint internal standard and multipoint external standard, several scholars have studied the determination of various mixtures. Stivenson established mathematical models using these two methods to detect and quantify both permanent gases and hydrocarbons.[48] In Alexander's research, the internal standard led to a highly accurate quantification. The external standard estimates the sensitivity factors by correlating MS signals to known gas concentrations via least-squares regressions.[49] Ghasemi used the GC/ECD method to study the QSRR of 38 diverse mixing substances; multiple linear regression and partial least-squares methods were used with leave-one-out cross-validation for developing the regression model. Comparing the regression analysis parameters, the two methods fit the results equally well.[50] In Sfetsas's study, GC/GC−TOFMS and GC-FID were used to determine the qualitative and quantitative analyses of 11 selected bio-oils; the measurement results are fitted to the weighted linear regression model, which provides publications addressing the issue of detailed quantification of bio-oils in an external standard.[51] Hunter analyzed the results of ethanol determination in beer by GC using the internal standard and external standard to assess the effectiveness of the analysis method and the calibration. They found that the internal standard can improve the correlation coefficient and decrease the percent relative error of the slope.[52] Currently however, there are few studies on the distortion of mixed gases' measurement results with the GC corrected by the calibration curve during a mine disaster period. In this paper, the problem is studied by the measurement experiments of multicomponent mixed gases with the multiple-point external standard in a large concentration gradient, and the least-squares method is used for fitting the linear calibration for multicomponent mixed gases.[53,54] Then, the calculation and correction models for the determination of multicomponent mixed gases during disaster and normal periods are established. Finally, this research provides a favorable environmental monitoring basis for mine disaster prevention and emergency rescue work in future applications.

2. EXPERIMENTAL SETUP AND SAMPLE PREPARATION

2.1. Experimental Setup. GC has great advantages and is widely used in determining the composition and concentration of multicomponent mixed gases. In this paper, the Agilent 490 portable gas chromatograph (Agilent 490GC) has been used to test the component concentration of the multicomponent mixed standard gases.

The Agilent 490GC is composed of four independent chromatographic column channels: micro-GC, electronic carrier gas control, a micro-machine sampler, a narrow-bore analytical column, and a micro thermal conductivity detector. The narrow-diameter capillary is used to measure gas components, greatly reducing the measurement time. The four independent analysis GC channels can be flexibly used in various environments and can be quickly reconfigured for different application conditions. In addition, the instrument can avoid the interference of other gases in the external environment through a microelectronic gas control device and an optional time-programmed backflush device. The physical diagram of Agilent 490GC is shown in Figure 1, the instrument test flow diagram is shown in Figure 2, and the measurement parameter settings are shown in Table 2.

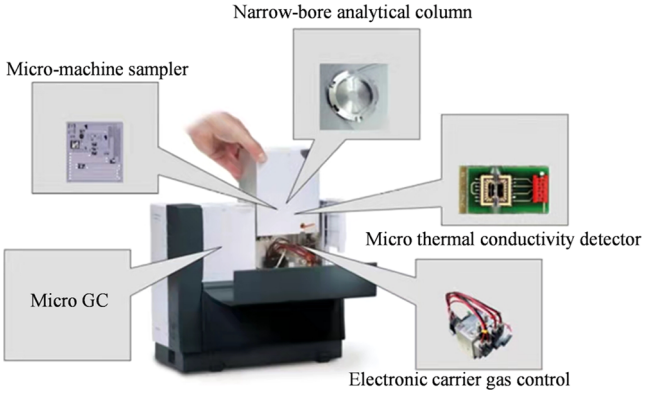

Figure 1. Physical diagram of Agilent 490 portable gas chromatograph (reprinted in part with permission from the user manual for the Agilent 490 portable gas chromatograph G3581-97001. Copyright 2017 Agilent Technologies, Inc.).

2.2. Preparation of Multicomponent Mixed-Gas Samples. To comprehensively simulate the composition of harmful gases in different mine disaster periods and avoid the deviation of the GC test results due to the instability of gases, this research uses multicomponent mixed gases with N_2 as the balance gas and contains different concentrations of H_2, O_2, CH_4, CO, CO_2, C_2H_4, C_2H_6, C_2H_2, and C_3H_8. These gases meet the national first-class gas standard; the composition and concentration of the 11 groups of multicomponent mixed standard gases used are shown in Table 3.

2.3. Reliability and Stability Test of Experimental Instrument. Before the component content determination experiment of the multicomponent mixed gas, the performance of the Agilent 490GC was tested to avoid large deviation in the measured results caused by instrumentation errors. The relative standard deviation of the gas peak area response value is determined by the multicomponent mixed gases 2# and 6#. The relative standard deviation of the measurement results is 0.06−0.9% and none of them exceeds 3%, as can be seen from Table 4 and Table 5. The measurement results meet the requirements of the JJG700-2019 "Gas Chromatograph Verification Regula-

https://doi.org/10.1021/acsomega.2c02391
ACS Omega 2022, 7, 25443−25457

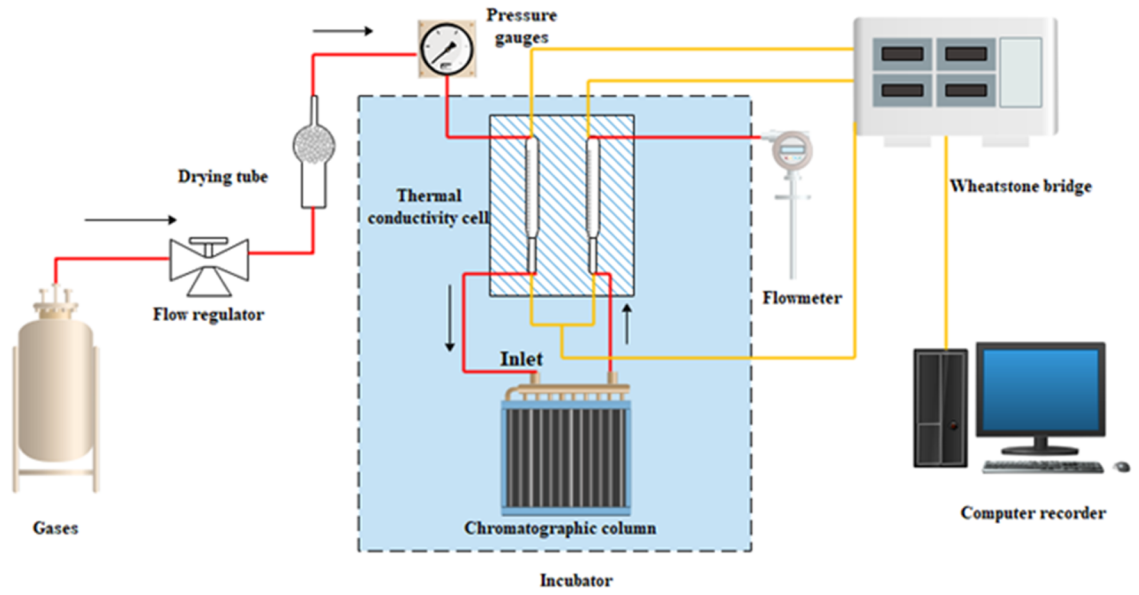

Figure 2. Test flow diagram of the Agilent 490 portable gas chromatograph.

Table 2. Agilent 490MicroGC Portable Gas Chromatograph Measurement Parameter Setting Table

aisle	carrier gas	column temperature (°C)	injection time (ms)	running time (s)	cylinder head pressure (kPa)	backflush time (s)
A	He	60	70	120	180	5
B	He	60	120	120	180	8

tions", so the Agilent 490GC has stable performance and strong reliability and meets the accuracy requirements.

3. EXPERIMENTAL PROTOCOL

In this paper, the composition and concentration of a standard multicomponent mixed gas are determined by Agilent 490GC. First, a specific gas (H_2, O_2, CH_4, etc.) in a set of standard gas samples (1#−11#) is selected as a reference component. Second, GC is used to measure the concentration of this component in other gas samples to obtain the response result. Third, this component in another standard gas sample is used as the reference component, and then, the concentration is measured in other gas samples. Finally, this kind of test is considered complete when this component in all gas samples is used as the reference component. Similarly, the concentration of another component is measured with this method. The response of reference components with different concentrations and types is obtained by GC. Finally, the response function between the measured results and the true concentration of different types and concentrations are established.

The specific operations for determining the components in the mixed gases are as follows: turn on the GC → preheat the instrument → select the standard gas → measure the standard gas → calibrate the standard gas sample → measure the gas concentrations of other groups; measure the various gas concentrations of each group in turn and analyze the measured results.

During the experiment, the measurement environment was as follows: 25 °C and 65 ± 15% RH. To reduce the influence of residual gases, the same group of gas was measured 3 times, and the last measurement result was used.

4. EXPERIMENTAL RESULTS AND ANALYSES

We selected H_2, O_2, CH_4, CO, CO_2, C_2H_4, C_2H_6, and C_2H_2 in turn, set the component as the reference component, and used GC to measure the concentration of this component in other standard gas samples. The measurement results of this gas

Table 3. Multicomponent Mixed-Gas Component Concentration Table (Unit: %)

	gas composition									
gas number	H_2	O_2	N_2	CH_4	CO	CO_2	C_2H_4	C_2H_6	C_2H_2	C_3H_8
1#	0.00928	0.509	7.38822	89.9	1.84	0.101	0	0.186	0.0665	0
2#	5.96	1	20.65	60	1.93	10	0.156	0.198	0.0809	0.0251
3#	0.0532	1.92	16.6927	79.3	1.53	0.249	0.00483	0.167	0.0557	0.0276
4#	4	3.08	46.6834	29.9	1.04	15	0.0811	0.154	0.041	0.0205
5#	0.104	3.65	23.7356	70.4	1.36	0.5	0.0305	0.135	0.052	0.0329
6#	2.03	5	52.3899	15.1	0.497	24.8	0.0417	0.106	0.0203	0.0151
7#	0.494	5.4	41.4424	50.2	1.24	0.963	0.0513	0.125	0.0463	0.038
8#	1.38	6.53	47.9965	40.4	1.07	2.39	0.061	0.0898	0.0407	0.042
9#	0.506	15.1	76.7847	2.5	0.0996	4.92	0.0199	0.05	0.00993	0.00991
10#	0	17.4	59.815	0.0979	0.0504	22.4	0.16	0.00465	0	0.0721
11#	0.0998	20.1	78.2746	0.986	0.0101	0	0.00998	0.00953	0.00502	0.00494

https://doi.org/10.1021/acsomega.2c02391
ACS Omega 2022, 7, 25443−25457

Table 4. Peak Area Response Value of Each Component Gas of Multicomponent Mixed Gas 2#

	gas composition								
serial number	H_2 ($\times10^4$)	O_2 ($\times10^5$)	N_2 ($\times10^7$)	CH_4 ($\times10^7$)	CO ($\times10^6$)	CO_2 ($\times10^6$)	C_2H_4 ($\times10^5$)	C_2H_6 ($\times10^5$)	C_2H_2 ($\times10^4$)
2#-1	4.79	7.97	1.46	3.55	1.37	9.64	1.53	2.03	6.51
2#-2	4.86	7.86	1.45	3.56	1.38	9.65	1.50	2.03	6.52
2#-3	4.82	7.87	1.46	3.56	1.38	9.65	1.50	2.03	6.52
2#-4	4.79	7.88	1.46	3.56	1.38	9.65	1.50	2.01	6.53
2#-5	4.86	7.88	1.46	3.56	1.38	9.66	1.50	2.03	6.53
2#-6	4.81	7.90	1.46	3.56	1.36	9.64	1.50	2.03	6.59
variance	0.34	0.41	0.01	0.04	0.07	0.08	0.0 1	0.01	0.0 31
average	4.82	7.89	1.46	3.56	1.37	9.65	1.51	2.03	6.53
relative standard deviation (%)	0.71	0.51	0.07	0.10	0.51	0.08	0.87	0.41	0.48

Table 5. Peak Area Response Value of Each Component Gas of Multicomponent Mixed Gas 6#

	gas composition								
serial number	H_2 ($\times10^4$)	O_2 ($\times10^6$)	N_2 ($\times10^7$)	CH_4 ($\times10^6$)	CO ($\times10^5$)	CO_2 ($\times10^7$)	C_2H_4 ($\times10^4$)	C_2H_6 ($\times10^4$)	C_2H_2 ($\times10^4$)
6#-1	1.91	2.99	3.19	7.87	3.04	2.13	3.87	9.20	1.44
6#-2	1.91	2.98	3.18	7.84	3.03	2.13	3.85	9.17	1.43
6#-3	1.90	2.98	3.18	7.84	3.04	2.11	3.85	9.19	1.43
6#-4	1.91	2.98	3.19	7.85	3.03	2.14	3.84	9.17	1.43
6#-5	1.92	2.98	3.18	7.84	3.03	2.14	3.85	9.19	1.43
6#-6	1.92	2.98	3.19	7.85	3.03	2.14	3.84	9.17	1.44
variance	0.01	0.00 4	0.0 2	0.0 1	0.00 5	0.0 1	0.01	0.0 1	0.00 4
average	1.91	2.98	3.18	7.84	3.03	2.13	3.85	9.18	1.44
relative standard deviation (%)	0.35	0.14	0.07	0.1 4	0.17	0.6	0.25	0.14	0.28

Table 6. H_2 Determination Concentration Table (Unit: %)

	substance (H_2)									
gas number	reference 1#	reference 2#	reference 3#	reference 4#	reference 5#	reference 6#	reference 7#	reference 8#	reference 9#	reference 11#
1#	0.00928	0.015434	0.00769	0.014709	0.00821	0.01409	0.01058	0.01304	0.01281	0.01068
2#	3.58347	5.96	1.92829	5.67982	3.16983	5.44066	4.08675	4.65003	4.94515	4.12324
3#	0.09062	0.16735	0.0532	0.1567	0.08745	1.02223	0.11275	0.12829	0.13643	0.11376
4#	2.52365	4.19732	1.358	4	2.23235	3.83157	2.87808	3.27477	3.48261	2.90378
5#	0.11757	0.19554	0.08327	0.18635	0.104	0.1785	0.07392	0.15256	0.16225	0.1 41 28
6#	1.33705	2.22377	0.71948	2.11923	1.18272	2.03	1.52483	1.735	1.84512	1.53845
7#	0.43316	0.72044	0.23309	0.68657	0.34232	0.65766	0.494	0.56209	0.59776	0.49841
8#	1.06347	1.40876	0.57226	1.49561	0.94072	1.61464	1.21283	1.38	1.46758	0.90366
9#	0.36667	0.57984	0.19731	0.58117	0.32435	0.5567	0.41817	0.4758	0.506	0.4219
11#	0.08674	0.14426	0.08467	0.13748	0.11062	0.13169	0.09892	0.11655	0.11969	0.0998

Table 7. H_2 Measurement Result Error Rate Table

	substance (H_2)									
gas number	refer to 1#	refer to 2#	refer to 3#	refer to 4#	refer to 5#	refer to 6#	refer to 7#	refer to 8#	refer to 9#	refer to 11#
1#	0	0.663147	0.171336	0.585022	0.115302	0.518319	0.140086	0.405172	0.380388	0.150862
2#	0.398747	0	0.676461	0.04701	0.468149	0.087138	0.314304	0.219794	0.170277	0.308181
3#	0.703383	2.145677	0	1.945489	0.643797	18.21485	1.119361	1.411466	1.564474	1.138346
4 #	0.369088	0.04933	0.6605	0	0.441913	0.042108	0.28048	0.181308	0.129348	0.274055
5 #	0.130481	0.880192	0.199327	0.791827	0	0.716346	0.289231	0.466923	0.560096	0.35846 2
6#	0.341355	0.095453	0.645576	0.043956	0.417379	0	0.248852	0.14532	0.091074	0.242143
7 #	0.123158	0.458381	0.07913	0.389818	0.143381	0.331296	0	0.137834	0.21004	0.008927
8#	0.22937	0.020841	0.585319	0.083775	0.318319	0.170029	0.121138	0	0.063464	0.345174
9#	0.275356	0.145929	0.610059	0.148557	0.358992	0.100198	0.173577	0.059684	0	0.166206
11#	0.130862	0.445491	0.151603	0.377555	0.108417	0.319539	0.008818	0.167836	0.199299	0

determined under different concentration reference components are obtained.

4.1. Analysis of H_2 Measured Results. We set H_2 in standard mixed gases 1#−9# and 11# as the reference component (the H_2 concentration of 10# is 0) and measured the H_2 concentration in other gas samples. From Table 6, it can be seen that the measured values deviate from the true values when we use different concentrations of H_2 reference components. To accurately measure the deviation between the measured value and the true value under different concen-

https://doi.org/10.1021/acsomega.2c02391
ACS Omega 2022, 7, 25443−25457

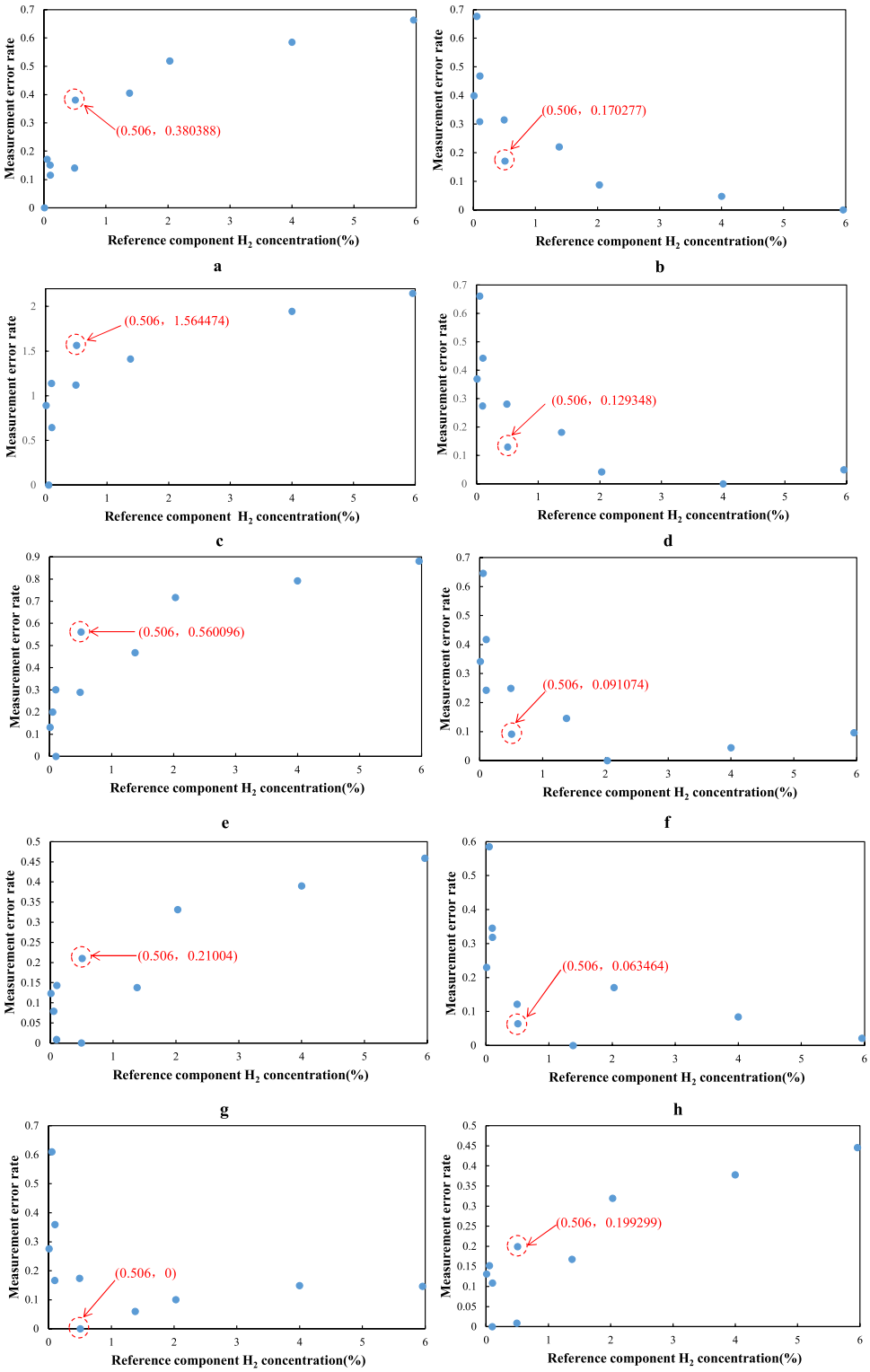

Figure 3. Scatter diagram of the measurement error rate of the H_2 content in each group of mixed gases under different concentrations of reference substances. (a) Measurement error rate of gas 1# with the concentration of 0.00928% at different concentrations of the reference component. (b) Measurement error rate of gas 2# with the concentration of 5.96% at different concentrations of the reference component. (c) Measurement error rate of gas 3# with the concentration of 0.0532% at different concentrations of the reference component. (d) Measurement error rate of gas 4# with the concentration of 4% at different concentrations of the reference component. (e) Measurement error rate of gas 5# with the concentration of 0.104% at different concentrations of the reference component. (f) Measurement error rate of gas 6# with the concentration of 2.03% at different concentrations of the reference component. (g) Measurement error rate of gas 7# with the concentration of 0.494% at different concentrations of the reference component. (h) Measurement error rate of gas 8# with the concentration of 1.38% at different concentrations of the reference component. (i) Measurement error rate of gas 9# with the concentration of 0.506% at different concentrations of the reference component. (j) Measurement error rate of gas 10# with the concentration of 0.0998% at different concentrations of the reference component.

https://doi.org/10.1021/acsomega.2c02391
ACS Omega 2022, 7, 25443−25457

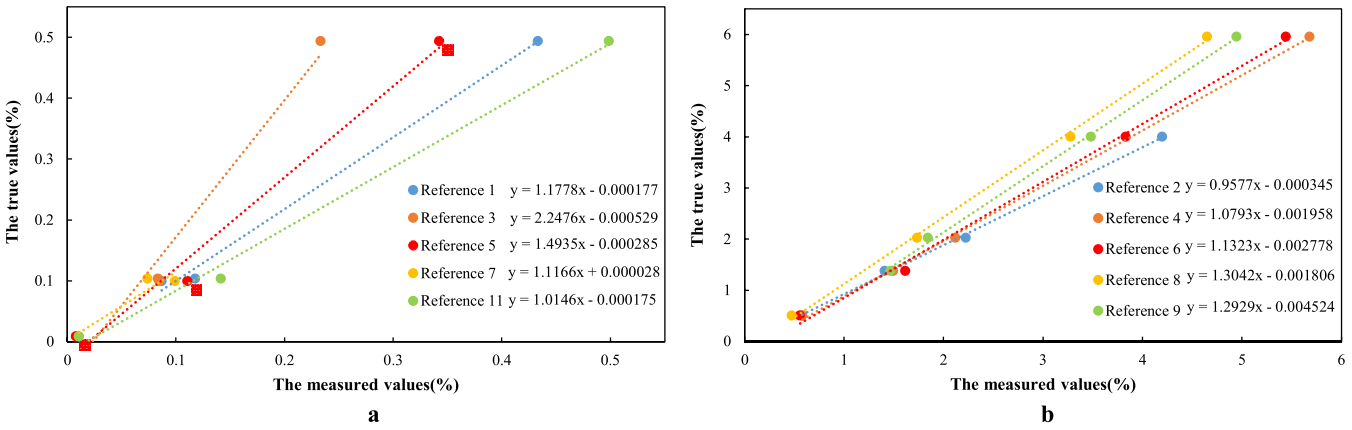

Figure 4. Fitting graph of the univariate linear regression between the measured concentration of H_2 and the true concentration in different concentration intervals. (a) Low-concentration H_2 measured and true value univariate linear regression fitting plot. (b) High-concentration H_2 measured and true value univariate linear regression fitting plot.

Table 8. Low-Concentration H_2 Univariate Linear Regression Analysis Parameter Table

	reference material				
fit metrics	reference 1#	reference 3#	reference 5#	reference 7#	reference 11#
coefficient of determination (r^2)	0.994937	0.947738	0.98389	0.902635	0.994204
residual sum of squares (SS_e)	0.000519	0.004875	0.00214	0.000558	0.000765

trations of H_2 reference components, the measured results are treated by the following formula

$$\eta = \frac{|a - b|}{b} \quad (1)$$

where a is the true concentration of H_2 in the standard gas sample, b is the measured value under different reference components, and η is the error rate of the measured value.

The error rate between the measured value and the true value of H_2 in other standard gas samples is shown in Table 7. It is found that the error rate of the measured value varies greatly with different concentrations of H_2 reference components. For example, the true concentration of H_2 in standard gas sample 1# is 0.00928%; when the standard gas sample 2# is chosen as the reference component (the H_2 concentration of 2# is 5.96%), the 1# measured value is 0.015434% and the error rate is as high as 0.663. However, when the standard gas sample 5# is chosen as the reference component (the H_2 concentration of 5# is 0.104%), the result is 0.00821%, with an error rate as low as 0.115.

It is found that the main influencing factors causing the error rate of the H_2 measured value are (1) the gas component to be measured, H_2 concentration, and (2) H_2 reference component concentration. To clear the trend of the error rate, the scatter diagram of 10 groups' standard mixed gases (1#−9#, 11#) under different concentrations of H_2 reference components is fitted in Figure 3. It is seen from Figure 3 that the error rate of the H_2 concentration measurement varies with the concentration of the H_2 reference component. The 10 kinds of standard gas samples can be divided into two categories according to the variation trend of the measured value error rate. (1) The gas samples represented in Figure 3a,3c,3e,3g,3j are classified as group A. When using a low-concentration H_2 reference component, the error rate of the measured value in this group is low. (2) The gas samples represented in Figure 3b,d,f,h,i are classified into group B. When using a high-concentration H_2 reference component, the error rate of the determination result in this group is low.

The H_2 concentration values in group A are 0.00928, 0.0532, 0.104, 0.494, and 0.0998%; the H_2 concentration values in group B are 5.96, 4, 2.03, 1.38, and 0.506%. The H_2 concentration values in group B are much higher than those in group A. For group A, when the low-concentration H_2 reference component is selected for measurements, the GC can accurately measure the concentration of H_2. However, when the concentration of the selected reference component is too high, the concentration difference between the reference component and group A becomes too large. There is a big deviation between the result of GC and the true value. For group B, when the high-concentration H_2 reference component is selected for measurements, the error rate of measurement results is low. However, when the concentration of the selected reference component (H_2) is too low, the GC cannot accurately determine the concentration of H_2, resulting in a large error rate. Therefore, selecting the appropriate concentration of reference components can effectively reduce the measurement error rate.

Based on Figure 3, the key point for the error rate of H_2 concentration determination is 0.506%. Hence, group A, where the H_2 concentration less than 0.506%, is called the low-concentration H_2 gas, and group B, where the H_2 concentration is greater than or equal to 0.506%, is called the high-concentration H_2 gas. The response characteristics of GC with different H_2 concentration ranges are determined, and then, the optimal response function of GC in different H_2 concentration ranges is obtained by comparing the response characteristic parameters.

Because the concentration of H_2 reference components has a great influence on the measured results, the measured values and the true values of H_2 in group A are fitted by linear regression when the low-concentration H_2 is selected as the reference component, as shown in Figure 4a. At the same time, we set the confidence level of the univariate linear regression fitting as 95%, and the coefficient of determination (r^2) and the residual sum of squares (SS_e) of the fitting model are calculated. When the r^2 is closer to 1 and the SS_e is closer to 0, the effect of univariate linear

https://doi.org/10.1021/acsomega.2c02391
ACS Omega 2022, 7, 25443−25457

Table 9. High-Concentration H_2 Univariate Linear Regression Analysis Parameter Table

	reference material				
fit metrics	reference 2#	reference 4#	reference 6#	reference 8#	reference 9#
coefficient of determination (r^2)	0.998646	0.999342	0.996652	0.998753	0.995988
residual sum of squares (SS_e)	0.008956	0.011466	0.062266	0.021032	0.014932

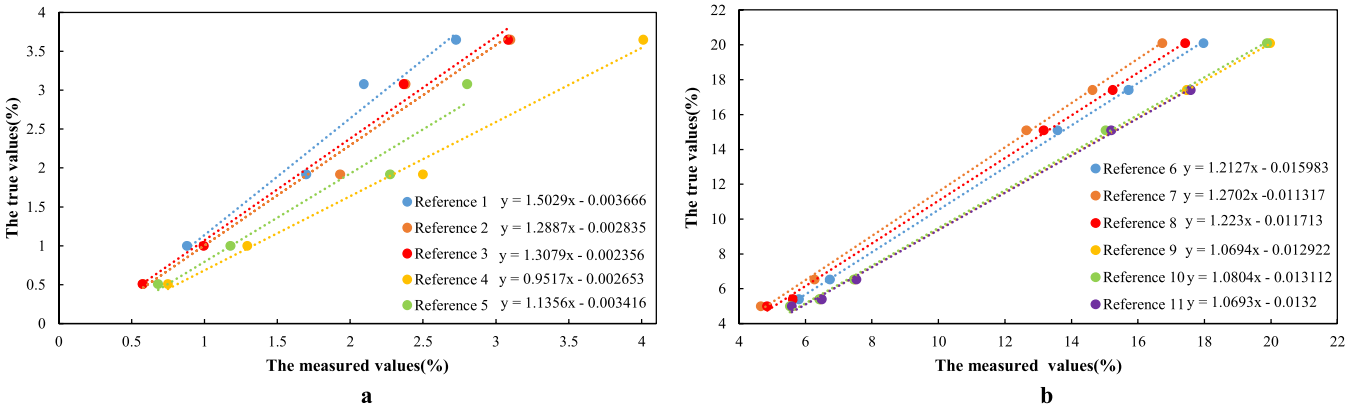

Figure 5. Fitting diagram of the univariate linear regression between the measured concentration of O_2 and the true concentration in different concentration intervals. (a) Low-concentration O_2 measured and true value univariate linear regression fitting plot. (b) High-concentration O_2 measured and true value univariate linear regression fitting plot.

regression analysis is better, and the corresponding fitting function is the optimal analysis function. Comparing the regression analysis parameters of group A (1#, 3#, 5#, 7#, 11#) in Table 8, it is found that when using gas 1# as the reference component, the regression analysis effect is found to be the best, and the fitting function is the optimal analysis function for the determination of low-concentration H_2.

When the high concentration of H_2 was chosen as the reference component, fitting the H_2 measured values and true values of group B as shown in Figure 4b. Through comparing the regression analysis parameters of group B (2#, 4#, 6#, 8#, 9#) in Table 9, when using gas 4# as the reference component, the regression analysis effect is found to be the best, and the fitting function is the optimal analysis function.

Therefore, when measuring low-concentration H_2 in the normal period of mines, standard gas sample 1# (the H_2 concentration is 0.00928%) is selected as the reference component. When measuring high-concentration H_2 during the disaster period, standard gas sample 4# (the H_2 concentration is 4%) is selected as the reference component. The optimal analysis function of GC in different H_2 concentration ranges is

$$y = 1.1778x - 0.000177,\ x < 0.506\%\ ;\ y = 1.0793x - 0.001958,\ x \geq 0.506\% \quad (2)$$

4.2. Analysis of O_2 Measured Results. We set O_2 in standard mixed gases 1#−11# as the reference component and measure the O_2 concentration in other gas groups. Due to the large amount of O_2 concentration (the actual O_2 concentration is 0.509−20.1%), the measured error of O_2 concentration is large. Similarly, the key point for the error rate of the O_2 concentration determination is 5%. The response characteristics of low-concentration O_2 gases are determined by the reference components with concentrations less than 5%, and the optimal response function of GC is determined in this concentration range. By the same method, the optimal response function of the high-concentration O_2 standard gas sample is determined using the reference component of the O_2 concentration greater than or equal to 5%.

The gas samples with low-concentration O_2 (1#, 2#, 3#, 4#, 5#) are classified as group C, and the gas samples with high-concentration O_2 (6#, 7#, 8#, 9#, 10#, 11#) are classified as group D. Setting the confidence level of the univariate linear regression fitting as 95%, the optimal analysis function is obtained by performing univariate linear regression analysis between the measured value and the true value of O_2 in different concentration ranges.

Figure 5 shows the fitting results of the univariate linear regression between the measured values and the true values of O_2. When measuring the group C gases, which represent the low-concentration O_2 during a disaster period in mines, gas sample 3# (the O_2 concentration is 1.92%) is used as the reference component. When measuring the group D gases, which represent the high-concentration O_2 during a normal period in mines, gas sample 6# (the O_2 concentration is 5%) is used as the reference component, and the univariate linear regression analysis effect is found to be the best. From this, the optimal analysis function of the GC in different O_2 concentration ranges is

$$y = 1.3079x - 0.002356,\ x < 5\%\ ;\ y = 1.2127x - 0.015983,\ x \geq 5\% \quad (3)$$

4.3. Analysis of CH_4 Measured Results. The key point for the error rate of the CH_4 concentration determination is 40.4%. The response characteristics of low-concentration CH_4 gases are determined by reference components with concentration less than 40.4%, and then, the optimal response function of GC is determined in this concentration range. By the same method, the optimal response function of high-concentration CH_4 standard gas samples is determined using the reference component of CH_4 concentration greater than or equal to 40.4%. The gas samples with low-concentration CH_4 (4#, 6#, 9#, 10#, 11#) are classified as group E, and the gas samples with high-concentration CH_4 (1#, 2#, 3#, 5#, 7#, 8#) are classified as

https://doi.org/10.1021/acsomega.2c02391
ACS Omega 2022, 7, 25443−25457

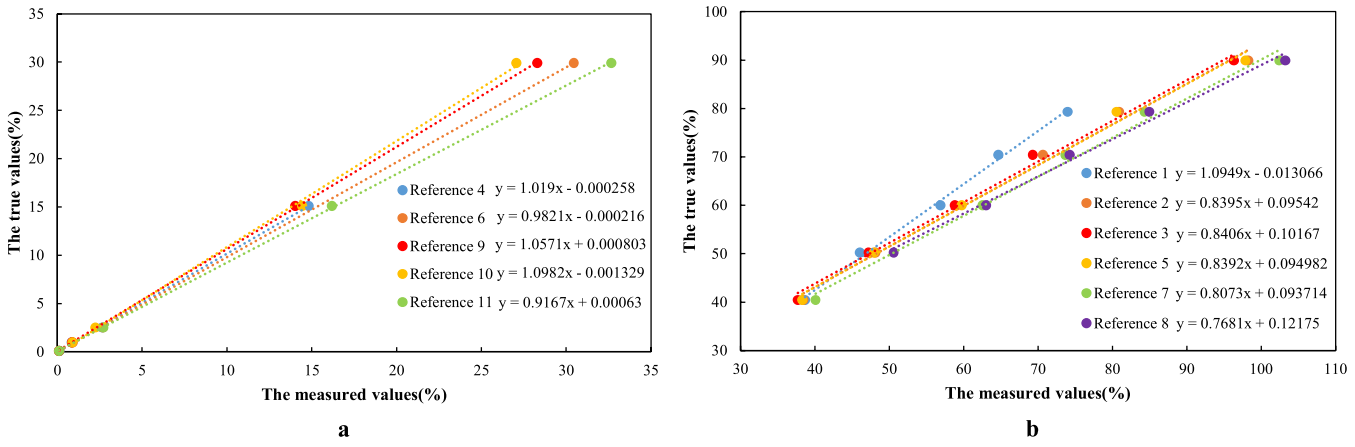

Figure 6. Fitting diagram of univariate linear regression between the measured concentration of CH_4 and the true concentration in different concentration intervals. (a) Low-concentration CH_4 measured and the true value univariate linear regression fitting plot. (b) High-concentration CH_4 measured and true value univariate linear regression fitting plot.

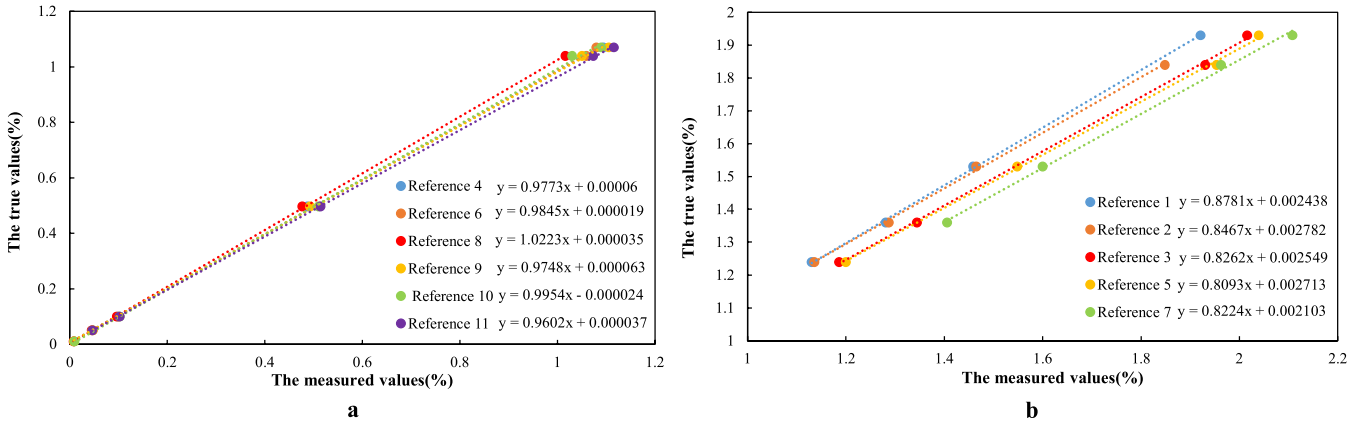

Figure 7. Fitting diagram of univariate linear regression between the measured concentration of CO and the true concentration in different concentration intervals. (a) Low-concentration CO measured and true value univariate linear regression fitting plot. (b) High-concentration CO measured and true value univariate linear regression fitting plot.

group F. Finally, the optimal analysis function is obtained by performing univariate linear regression analysis between the measured value and the true value of CH_4 in different concentration ranges.

Figure 6 shows the fitting results of the univariate linear regression with different CH_4 concentration ranges. When measuring the group E gases, which represent the low-concentration CH_4 in the normal period, gas sample 6# (the CH_4 concentration is 15.1%) is used as the reference component. When measuring the group F gases, which represent the high-concentration CH_4 during a disaster period, gas sample 1# (the CH_4 concentration is 89.9%) is used as the reference component. On this basis, the univariate linear regression analysis effect between the measured values and the true value is found to be the best. From this, the optimal analysis function of the GC in different CH_4 concentration ranges is

$$y = 0.9821x - 0.000216,\ x < 40.4\% \quad ;\ y = 1.0949x - 0.013066,\ x \geq 40.4\% \tag{4}$$

4.4. Analysis of CO Measured Results. The key point for the error rate of the CO concentration determination is 1.24%. The response characteristics of low-concentration CO gases are determined by reference components with concentration less than 1.24%, and then, the optimal response function of GC is determined in this concentration range. By the same method, the optimal response function of high-concentration CO standard gas samples is determined using the reference component of the CO concentration greater than or equal to 1.24%. The gas samples with low-concentration CO (4#, 6#, 8#, 9#, 10#, 11#) are classified as group G, and the gas samples with high-concentration CO (1#, 2#, 3#, 5#, 7#) are classified as group H. Finally, the optimal analysis function is obtained by performing univariate linear regression analysis between the measured value and the true value of CO in different concentration ranges.

Figure 7 shows the fitting results of the univariate linear regression with different CO concentration ranges. When measuring the group G gases, which represent the low-concentration CO in the normal period, gas sample 6# (the CO concentration is 0.497%) is used as the reference component. When measuring the group F gases, which represent the high-concentration CO during a disaster period, gas sample 1# (the CO concentration is 1.84%) is used as the reference component. On this basis, the univariate linear regression analysis effect between the measured values and the true value was found to be the best. From this, the optimal analysis function of the GC in different CO concentration ranges is found to be

https://doi.org/10.1021/acsomega.2c02391
ACS Omega 2022, 7, 25443−25457

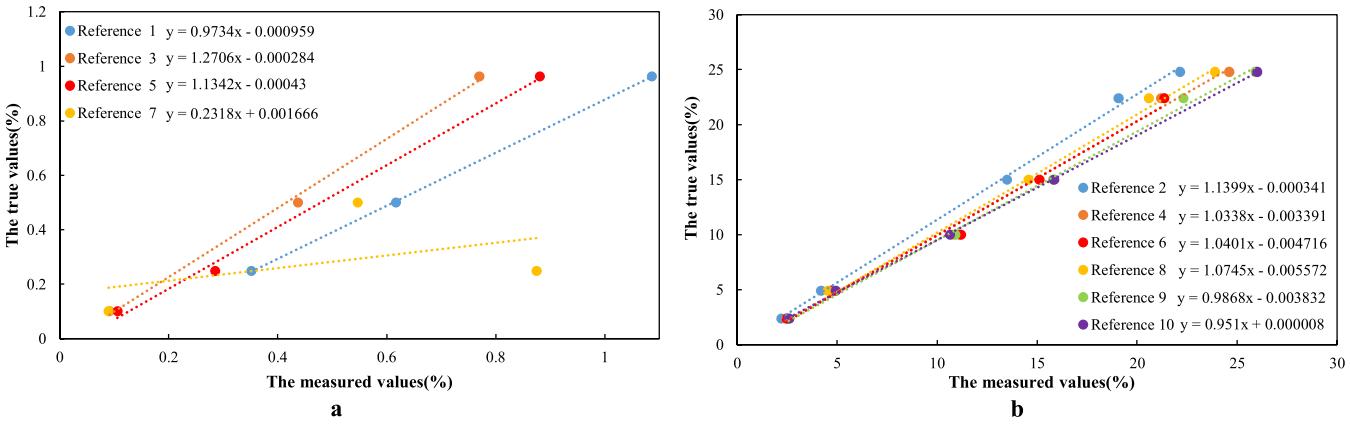

Figure 8. Fitting diagram of univariate linear regression between the measured concentration of CO_2 and the true concentration in different concentration intervals. (a) Low-concentration CO_2 measured and true value univariate linear regression fitting plot. (b) High-concentration CO_2 measured and true value univariate linear regression fitting plot.

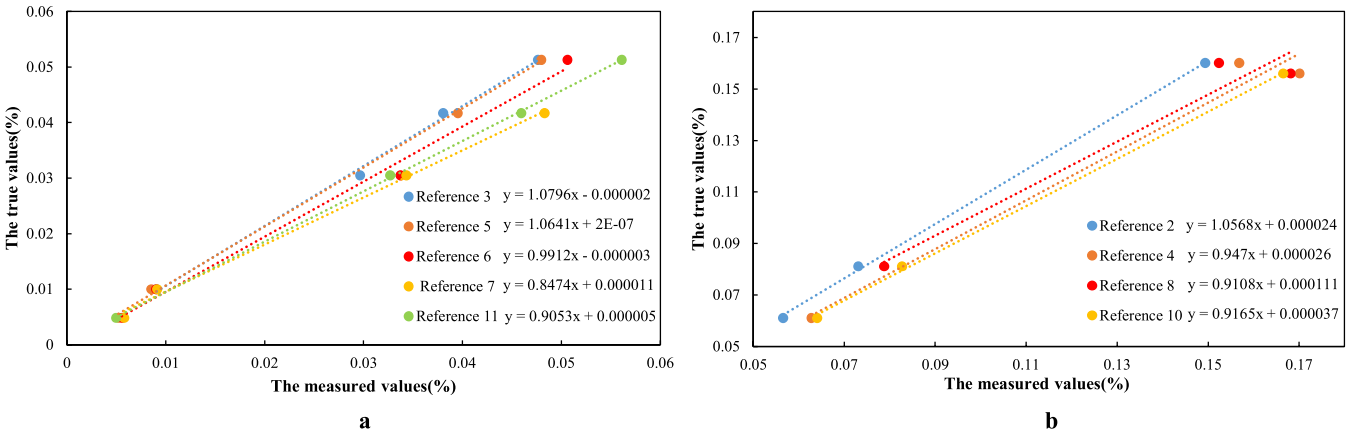

Figure 9. Fitting diagram of linear univariate linear regression between the measured concentration of C_2H_4 and the true concentration in different concentration intervals. (a) Low-concentration C_2H_4 measured and true value univariate linear regression fitting plot. (b) High-concentration C_2H_4 measured and true value univariate linear regression fitting plot.

$$y = 0.9845x + 0.000019,\ x < 1.24\%$$
$$;\ y = 0.8781x + 0.002438,\ x \geq 1.24\% \quad (5)$$

4.5. Analysis of CO_2 Measured Results. The key point for the error rate of the CO_2 concentration determination is 2.39%. The response characteristics of low-concentration CO_2 gases are determined by reference components with concentration less than 2.39%, and then, the optimal response function of GC is determined in this concentration range. By the same method, the optimal response function of high-concentration CO_2 standard gas samples is determined using the reference component of CO_2 concentration greater than or equal to 2.39%. The gas samples with low-concentration CO_2 (1#, 3#, 5#, 7#) are classified as group I, and the gas samples with high-concentration CO_2 (2#, 4#, 6#, 8#, 9#, 10#) are classified as group J. Finally, the optimal analysis function is obtained by performing univariate linear regression analysis between the measured value and the true value of CO_2 in different concentration ranges.

Figure 8 shows the fitting results of the univariate linear regression with different CO_2 concentration ranges. When measuring the group I gases, which represent the low-concentration CO_2 in the normal period, gas sample 1# (the CO_2 concentration is 0.101%) is used as the reference component. When measuring the group J gases, which represent the high-concentration CO_2 during the disaster period, gas sample 10# (the CO_2 concentration is 22.4%) is used as the reference component. On this basis, the univariate linear regression analysis effect between the measured values and the true value is found to be the best. From this, the optimal analysis function of the GC in different CO_2 concentration ranges is

$$y = 0.9734x - 0.000959,\ x < 2.39\%$$
$$;\ y = 0.951x + 0.000008,\ x \geq 2.39\% \quad (6)$$

4.6. Analysis of C_2H_4 Measured Results. The key point for the error rate of the C_2H_4 concentration determination is 0.061%. The response characteristics of low-concentration C_2H_4 gases are determined by reference components with concentration less than 0.061%, and then, the optimal response function of GC is determined in this concentration range. By the same method, the optimal response function of high-concentration C_2H_4 standard gas samples is determined using the reference component of the C_2H_4 concentration greater than or equal to 0.061%. The gas samples with low-concentration C_2H_4 (3#, 5#, 6#, 7#, 9#, 11#) are classified as group K, and the gas samples with high-concentration C_2H_4 (2#, 4#, 8#, 10#) are classified as group L. Finally, the optimal analysis function is obtained by performing univariate linear regression analysis

https://doi.org/10.1021/acsomega.2c02391
ACS Omega 2022, 7, 25443−25457

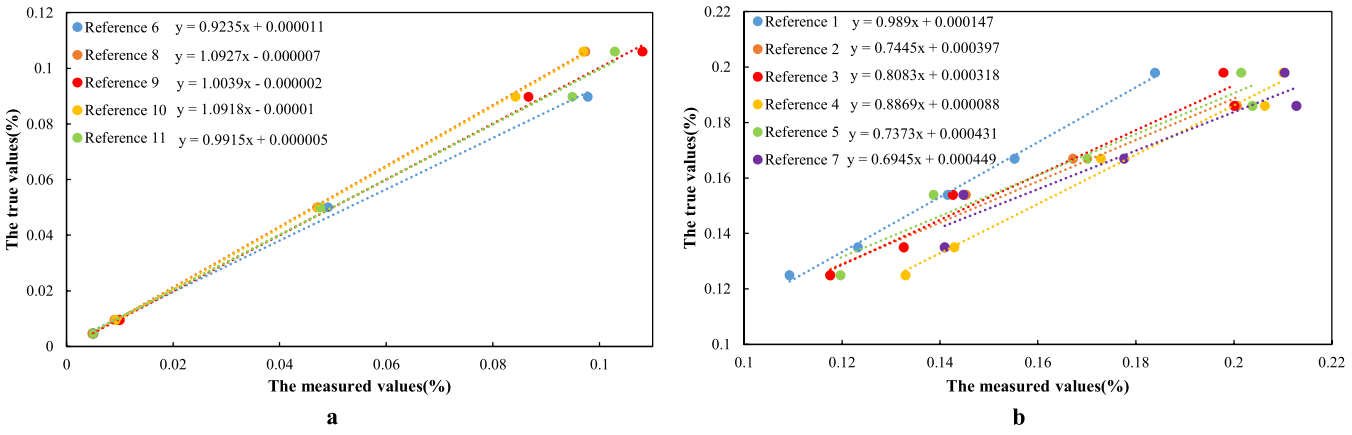

Figure 10. Fitting diagram of linear univariate linear regression between the measured concentration of C_2H_6 and the true concentration in different concentration intervals. (a) Low-concentration C_2H_6 measured and true value univariate linear regression fitting plot. (b) High-concentration C_2H_6 measured and true value univariate linear regression fitting plot.

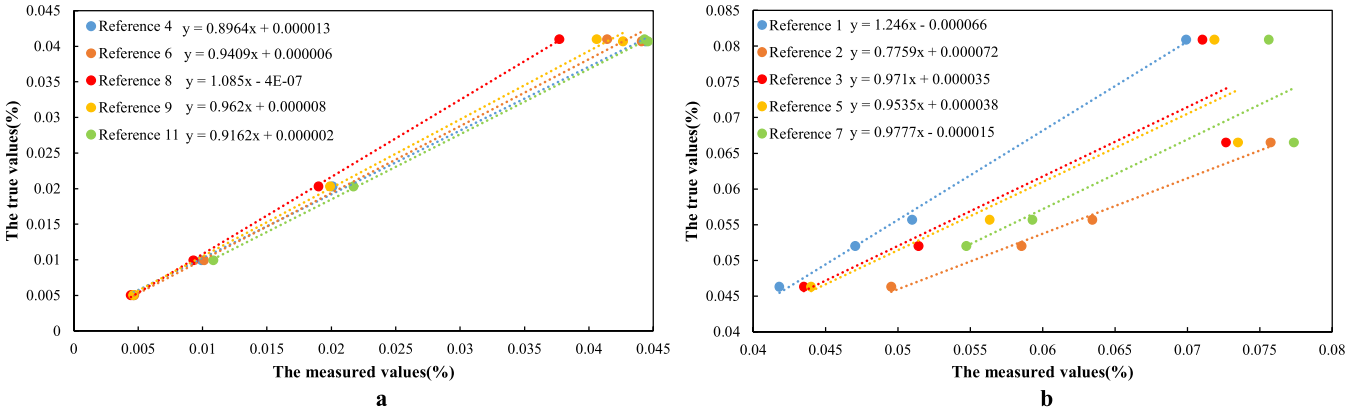

Figure 11. Fitting diagram of linear univariate linear regression between the measured concentration of C_2H_2 and the true concentration in different concentration intervals. (a) Low-concentration C_2H_2 measured and true value univariate linear regression fitting plot. (b) High-concentration C_2H_2 measured and true value univariate linear regression fitting plot.

between the measured value and the true value of C_2H_4 in different concentration ranges.

Figure 9 shows the fitting results of the univariate linear regression with different C_2H_4 concentration ranges. When measuring the group K gases, which represent the low-concentration C_2H_4 in the normal period, gas sample 11# (the C_2H_4 concentration is 0.00998%) is used as the reference component. When measuring the group L gases, which represent the high-concentration C_2H_4 during the disaster period, gas sample 2# (the C_2H_4 concentration is 0.156%) is used as the reference component. On this basis, the univariate linear regression analysis effect between the measured values and the true value is found to be the best. From this, the optimal analysis function of the GC in different C_2H_4 concentration ranges is

$$y = 0.9053x + 0.000005,\ x < 0.061\%\ ;\ y = 1.0568x + 0.000024,\ x \geq 0.061\% \quad (7)$$

4.7. Analysis of C_2H_6 Measured Results. The key point for the error rate of the C_2H_6 concentration determination is 0.125%. The response characteristics of low-concentration C_2H_6 gases are determined by reference components with concentration less than 0.125%, and then, the optimal response function of GC is determined in this concentration range. By the same method, the optimal response function of high-concentration C_2H_6 standard gas samples is determined using the reference component of C_2H_6 concentration greater than or equal to 0.125%. The gas samples with low-concentration C_2H_6 (6#, 8#, 9#, 10#, 11#) are classified as group M, and the gas samples with high-concentration C_2H_6 (1#, 2#, 3#, 4#, 5#, 7#) are classified as group N. Finally, the optimal analysis function is obtained by performing univariate linear regression analysis between the measured value and true value of C_2H_6 in different concentration ranges.

Figure 10 shows the fitting results of the univariate linear regression with different C_2H_6 concentration ranges. When measuring the group M gases, which represent the low-concentration C_2H_6 in the normal period, gas sample 8# (the C_2H_6 concentration is 0.0898%) is used as the reference component. When measuring the group N gases, which represent the high-concentration C_2H_6 during the disaster period, gas sample 1# (the C_2H_6 concentration is 0.186%) is used as the reference component. On this basis, the univariate linear regression analysis effect between the measured values and the true value is found to be the best. From this, the optimal analysis function of the GC in different C_2H_6 concentration ranges is

$$y = 1.0927x - 0.000007,\ x < 0.125\%\ ;\ y = 0.989x + 0.000147,\ x \geq 0.125\% \quad (8)$$

https://doi.org/10.1021/acsomega.2c02391
ACS Omega 2022, 7, 25443−25457

Table 10. Error Rate Table between the Measured Results of Each Gas and the True Value after the Calibration of the Optimal Analytical Function

	gas composition							
serial number	H_2	O_2	CH_4	CO	CO_2	C_2H_4	C_2H_6	C_2H_2
1#		0.016143						
2#	0.00429	0.065482	0.016151	0.000367	0.012505	0	0.007176	0.004786
3#	0.673538		0.00507	0.003732	0.011282	0.033561	0.007296	0.021766
4#		0.071385	0.000285	0.004632	0.005251	0.018075	0.004635	0.034804
5#	0.161287	0.040054	0.013045	0.006435	0.008817	0.013837	0.011611	0.000347
6#	0.030288				0.00265	0.009145	0.003206	
7#	0.003085	0.006277	0.021753	0.003021	0.001634	0.000265	0.017872	0.017542
8#	0.027835	0.005974	0.015739	0.004465	0.035465	0.019639		0.033919
9#	0.147319	0.014973	0.048436	0.012077	0.045415		0.0141	0.019989
10#		0.003527	0.095432	0.039489		0.001615	0.01648	
11#	0.15368 4	0.00454	0.105818	0.064421			0.039687	0.001055

4.8. Analysis of C_2H_2 Measured Results. The key point for the error rate of the C_2H_2 concentration determination is 0.0463%. The response characteristics of low-concentration C_2H_2 gases are determined by reference components with concentration less than 0.0463%, and then, the optimal response function of GC is determined in this concentration range. By the same method, the optimal response function of high-concentration C_2H_2 standard gas samples is determined using the reference component of C_2H_2 concentration greater than or equal to 0.0463%. The gas samples with low-concentration C_2H_2 (4#, 6#, 8#, 9#, 11#) are classified as group O, and the gas samples with high-concentration C_2H_2 (1#, 2#, 3#, 5#, 7#) are classified as group P. Finally, the optimal analysis function is obtained by performing univariate linear regression analysis between the measured value and the true value of C_2H_2 in different concentration ranges.

Figure 11 shows the fitting results of the univariate linear regression with different C_2H_2 concentration ranges. When measuring the group O gases, which represent the low-concentration C_2H_2 in the normal period, gas sample 6# (the C_2H_2 concentration is 0.0203%) is used as the reference component. When measuring the group P gases, which represent the high-concentration C_2H_2 during the disaster period, gas sample 1# (the C_2H_2 concentration is 0.0665%) is used as the reference component. On this basis, the univariate linear regression analysis effect between the measured values and the true value is found to be the best. From this, the optimal analysis function of the GC in different C_2H_2 concentration ranges is

$$y = 0.9409x + 0.000006,\ x < 0.0463\%;\quad y = 1.246x - 0.000066,\ x \geq 0.0463\% \tag{9}$$

Meanwhile, the optimal reference component concentration should be selected as follows. (1) During the normal period, H_2 is 0.00928%, O_2 is 5%, CH_4 is 15.1%, CO is 0.497%, CO_2 is 0.101%, C_2H_4 is 0.00998%, C_2H_6 is 0.0898%, and C_2H_2 is 0.0203%. (2) During the disaster period, H_2 is 4%, O_2 is 1.92%, CH_4 is 89.9%, CO is 1.84%, CO_2 is 22.4%, C_2H_4 is 0.156%, C_2H_6 is 0.186%, and C_2H_2 is 0.0665%.

5. DISCUSSION

Compared with experiments of other studies of mixing gases' determination, most of them used an internal standard or external standard calibration instrument and correlated the reaction signal with the known gas concentration to accurately quantify the mixed gases via the least-squares method.[49,55−57] Velasco-Rozo analyzed the advantages of the internal standard and the external standard for the related experimental setup.[49] To tackle the effect that the concentration and nature of the components of the effluent change over time due to the catalytic reaction, the corresponding mathematical models based on the internal standard and the external standard were established.[48] In addition, Ghasemi established the optimal fitting model for determining the results of multiple mixtures based on multiple linear regression and partial least-squares projections to latent structures, providing a sound theoretical basis.[51] However, currently, there are few studies on the distortion of mixed gases' measurement results with the GC corrected by the calibration curve. Thus, this paper conducts an in-depth study on this problem. In this paper, 11 groups of mixed gases were determined by calibrated GC. It was found that the error rates of the measured results have a strong correlation with the concentration of the selected reference component and the component to be measured. The key point of each gas is determined by the error scatter diagram, which divides each gas into different concentration groups. Each gas is selected as the reference component to measure the concentration of the corresponding component in other gases with the multiple-point external standard, and the least-squares method is used for linear fitting between measured values and true values. The optimal analysis function is obtained by comparing the regression analysis parameters in different concentration ranges. Calibration of the measured results using these optimal analysis functions is shown in Table 10. It is found that the error rate of measured values corrected by the optimal analysis function is far less than the uncorrected one. It shows the reliability of this method. Therefore, the method not only can alleviate the distortion of the measured results during the disaster period but also can provide powerful environmental monitoring guarantee for mine disaster prevention and rescue work.

6. CONCLUSIONS

To solve the problem of distortion of measurement results by GC, the GC corrected by the calibration curve is used to determine the concentration of 11 groups of mixed gases. It was found that the difference in the error rate of measured results is related to the concentration of the selected reference component and the component to be measured. Every gas is divided into a high- and a low-concentration group by the key points. Compared with the study of the relationship between the reaction signal and the true concentration in mixed gases, the

https://doi.org/10.1021/acsomega.2c02391
ACS Omega 2022, 7, 25443−25457

multiple-point external standard is used to correlate the measured values and the true values in different concentration groups. Then, the optimal analysis function of each gas can be determined by the least-squares method during the mine disaster period. This method provides a new idea and a practical basis for accurately determining mixed gases. It has far-reaching influence on mine disaster prevention and rescue work. The relevant detailed conclusions are as follows.

(1) Through the experimental results, a large error between the measured result and the true value of the gas concentration was found. The main reason for this is that the concentration difference between the gas to be measured and the reference component is too large.

(2) According to the measurement error rate scatter diagrams of standard multicomponent mixed gases, the key point for distinguishing high and low concentrations is determined. In this research, the key points for each gas concentration are as follows: H_2 is 0.506%, O_2 is 5%, CH_4 is 40.4%, CO is 1.24%, CO_2 is 2.39%, C_2H_4 is 0.061%, C_2H_6 is 0.125%, and C_2H_2 is 0.0463%.

(3) Every standard multicomponent mixed gases is divided into high and low concentration groups by the key points; the high- and low-concentration gases are selected as the reference components to fit univariate linear regression analysis between the measured results and the true values of gases in the corresponding concentration range. Comparing the r^2 and SS_e, the optimal analysis function and the reference component concentration in different concentration ranges can be determined.

(4) Through calibration of measured results using these optimal analysis functions, it is found that the error rate between the calibration result and the true value is much less than the result without calibration. This proves the reliability and superiority of the method, and the method can provide strong support for mine disaster prevention, hazard identification, and rescue work.

AUTHOR INFORMATION

Corresponding Author

Chenchen Wang − *School of Emergency Management and Safety Engineering, China University of Mining and Technology (Beijing), Beijing 100083, China;* orcid.org/0000-0002-7089-8245; Email: cumtbwangchenchen@126.com

Authors

Feng Li − *School of Emergency Management and Safety Engineering, China University of Mining and Technology (Beijing), Beijing 100083, China*

Yue Zhang − *CNOOC Energy Development Co., Ltd., Beijing 100028, China*

Xiaoxuan He − *School of Emergency Management and Safety Engineering, China University of Mining and Technology (Beijing), Beijing 100083, China*

Chenyu Zhang − *School of Emergency Management and Safety Engineering, China University of Mining and Technology (Beijing), Beijing 100083, China*

Fangfei Sha − *Xuchang Cigarette Factory of China Tobacco Tenants Industrial Co., Ltd., Xuchang 461001 Henan, China*

Complete contact information is available at: https://pubs.acs.org/10.1021/acsomega.2c02391

Notes

The authors declare no competing financial interest.

All data included in this study are available upon request by contact with the corresponding author.

ACKNOWLEDGMENTS

This research was conducted with financial support from the National Natural Science Foundation of China (52064046 and 51804311), the Department of Science and Technology of Xinjiang Uygur Autonomous Region (Science and Technology Aid Xinxiang) (2020E0258), the China Scholarship Council (CSC), and the Fundamental Research Funds for the Central Universities (2020YJSAQ13).

REFERENCES

(1) Du, W. Z.; Zhang, J.; Xie, Q. X.; Zhang, Y. S.; Niu, K.; Wang, H. W. Experimental study on optimizing the inhibition effect of pre-injection inhibitor on coal spontaneous combustion. *Energy Sources, Part A* **2020**, 1−18.

(2) Lu, W.; Guo, B. L.; Qi, G. S.; Cheng, W. M.; Yang, W. Y. Experimental study on the effect of preinhibition temperature on the spontaneous combustion of coal based on an $MgCl_2$ solution. *Fuel* **2020**, *265*, No. 117032.

(3) Nimaje, D. S.; Tripathy, D. P. Characterization of some Indian coals to assess their liability to spontaneous combustion. *Fuel* **2016**, *163*, 139−147.

(4) Lu, W.; Cao, Y. J. Z.; Tien, J. C. Method for prevention and control of spontaneous combustion of coal seam and its application in mining field. *Int. J. Min. Sci. Technol.* **2017**, *27*, 839−846.

(5) Ren, X. W.; Wang, F. Z.; Guo, Q.; Zuo, Z. B.; Fang, Q. S. Application of foam-gel technique to control CO exposure generated during spontaneous combustion of coal in coal mines. *J. Occup. Environ. Hyg.* **2015**, *12*, D239−D245.

(6) Hricov, R.; Šenk, A.; Kroha, P.; Valenta, M. Evaluation of Xpath queries over XML documents using sparkSQL framework. Beyond Databases, Architectures and Structures. Towards Efficient Solutions for Data Analysis and Knowledge Representation. BDAS. *Commun. Comput. Inf. Sci.* **2017**, *716*, 28−41.

(7) Si, L. L.; Wei, J. P.; Xi, Y. J.; Wang, H. Y.; Wen, Z. H.; Li, B.; Zhang, H. T. The influence of long-time water intrusion on the mineral and pore structure of coal. *Fuel* **2021**, *290*, No. 119848.

(8) Song, Z. Y.; Kuenzer, C. Coal fires in China over the last decade: A comprehensive review. *Int. J. Coal Geol.* **2014**, *133*, 72−99.

(9) Onifade, M.; Genc, B. A review of research on spontaneous combustion of coal. *Int. J. Min. Sci. Technol.* **2020**, *30*, 303−311.

(10) Brodny, J.; Tutak, M. Determination of the zone with a particularly high risk of endogenous fires in the goaves of a longwall with caving. *J. Appl. Fluid Mech.* **2018**, *11*, 545−553.

(11) Zhang, J.; Zhang, H. T.; Ren, T.; Wei, J. P.; Liang, Y. T. Proactive inertisation in longwall goaf for coal spontaneous combustion control-A CFD approach. *Saf. Sci.* **2019**, *113*, 445−460.

(12) Qiao, M.; Ting, R.; Jon, R.; Xiaohan, Y.; Zhongbei, L.; Jianming, W. New insight into proactive goaf inertisation for spontaneous combustion management and control. *Process Saf. Environ. Prot.* **2022**, *161*, 739−757.

(13) Li, L.; Qin, B. T.; Liu, J. S.; Leong, Y. K.; Li, W.; Zeng, J.; Ma, D.; Zhuo, H. Influence of airflow movement on methane migration in coal mine goafs with spontaneous coal combustion. *Process Saf. Environ. Prot.* **2021**, *156*, 405−416.

(14) Wang, H.; Dlugogorski, B. Z.; Kennedy, E. M. Analysis of the mechanism of the low-temperature oxidation of coal. *Combust. Flame* **2003**, *134*, 107−117.

(15) Wang, D. M.; Xin, H. H.; Qi, X. Y.; Dou, G. L.; Qi, G. S.; Ma, L. Y. Reaction pathway of coal oxidation at low temperatures: a model of cyclic chain reactions and kinetic characteristics. *Combust. Flame* **2016**, *163*, 447−460.

(16) Xiao, Y.; Ren, S. J.; Deng, J.; Shu, C. M. Comparative analysis of thermokinetic behavior and gaseous products between first and second coal spontaneous combustion. *Fuel* **2018**, *227*, 325−333.
(17) Wang, J. F.; Zhang, Y. L.; Xue, S.; Wu, J. M.; Tang, Y. B.; Chang, L. P. Assessment of spontaneous combustion status of coal based on relationships between oxygen consumption and gaseous product emissions. *Fuel Process. Technol.* **2018**, *179*, 60−71.
(18) Xu, Q.; Yang, S. Q.; Tang, Z. Q.; Cai, J. W.; Zhong, Y.; Zhou, B. Z. Free radical and functional group reaction and index gas CO emission during coal spontaneous combustion. *Combust. Sci. Technol.* **2018**, *190*, 834−848.
(19) Jiang, X. Y.; Yang, S. Q.; Zhou, B. Z.; Hou, Z. S.; Zhang, C. S. Effect of gas atmosphere change on radical reaction and indicator gas release during coal oxidation. *Fuel* **2022**, *312*, No. 122960.
(20) Liang, Z.; Wang, J. R. In the technology of forecasting and predicting the hidden danger of underground coal spontaneous combustion. *Procedia Eng.* **2011**, *26*, 2301−2305.
(21) Deng, J.; Chen, W. L.; Liang, C.; Wang, W. F.; Xiao, Y.; Wang, C. P.; Shu, C. M. Correction model for CO detection in the coal combustion loss process in mines based on GWO-SVM. *J. Loss Prev. Process Ind.* **2021**, *71*, No. 104439.
(22) Jiang, X. Y.; Yang, S. Q.; Zhou, B. Z.; Song, W. X.; Cai, J. W.; Xu, Q.; Zhou, Q. C.; Yang, K. The variations of free radical and index gas CO in spontaneous combustion of coal gangue under different oxygen concentrations. *Fire Mater.* **2022**, *46*, 549−559.
(23) Wen, H.; Liu, Y.; Guo, J.; Jin, Y. F.; Zheng, X. Z. A multi-index-classified early warning method for spontaneous combustion of coal under air leakage blocking. *Int. J. Oil, Gas Coal Technol.* **2021**, *27*, 208−226.
(24) Guo, X. Y.; Deng, C. B.; Zhang, X.; Wang, Y. S. Formation law of hydrocarbon index gases during coal spontaneous combustion in an oxygen-poor environment. *Energy Sources, Part A* **2019**, *41*, 626−635.
(25) Hu, X. C.; Yang, S. Q.; Zhou, X. H.; Yu, Z. Y.; Hu, C. Y. Coal spontaneous combustion prediction in gob using chaos analysis on gas indicators from upper tunnel. *J. Nat. Gas Sci. Eng.* **2015**, *26*, 461−469.
(26) Miao, G. D.; Li, Z. H.; Meng, Q. X.; Li, J. H.; Yang, Y. L. Experimental research on the emission of higher molecular weight gases during coal oxidation. *Fuel* **2021**, *300*, No. 120906.
(27) Kuchta, J. M.; Furno, A. L.; Dalverny, L. E.; Sapko, M. J.; Litton, C. D.Diagnostics of Sealed Coal Mine Fires. *Report of Investigations*, 1982, pp 15−25.
(28) Feiler, J. J.; Colaizzi, G. J.; Carder, C. Foamed grout controls underground coal-mine fire. *Min. Eng.* **2000**, *52*, 58−62.
(29) Zhou, X.; Le, M.; Meijing, S.; Lianghui, G.; Jianyuan, Z.; Cuncun, F. Influences of sealing fire zone in high gas mine on impact factors of gas explosion limits. *Baozha Yu Chongji* **2013**, *33*, 351−356.
(30) Zhou, F.; Jinhai, L. Prediction model for reignition of fire zone after unsealing based on BP neural networks. *J. Min. Saf. Eng.* **2010**, *27*, 494−498.
(31) Wang, C. J.; Yang, S. Q.; Li, X. W. Simulation of the hazard arising from the coupling of gas explosions and spontaneously combustible coal due to the gas drainage of a gob. *Process Saf. Environ. Prot.* **2018**, *118*, 296−306.
(32) Liu, Y.; Haibo, C. Poison gases propagation rules of methane explosion in coal mine. *Meitan Xuebao* **2009**, *34*, 788−791.
(33) Jia, Z.; Guoxun, J.; Qiang, Z. Analysis on the diffusion of toxic gases from gas explosion and the determination of risk area. *Zhongguo Anquan Kexue Xuebao* **2007**, *17*, 91−95.
(34) *Coal Mine Safety Regulations*; Emergency Management Press: Beijing, 2022; p 411.
(35) Zujing, Z.; Lin, L.; Kequan, W. Causes of rescuers death in mine emergency rescue and strtegies. *China Coal* **2016**, *42*, 88−91.
(36) Haiying, Q. Discussion on present situation and development trend of mine disaster reconnaissance technology and equipment. *Min. Saf. Environ. Prot.* **2015**, *42*, 116−118.
(37) Schon, H. G.; Gruhn, G.; Neumann, W. Quantitative-analysis of the availibility of chemical-plants by simulation methods. *Chem. Technol.* **1980**, *32*, 177−181.
(38) Langelaan, D. N.; Reddy, T.; Banks, A. W.; Dellaire, G.; Dupre, D. J.; Rainey, J. K. Structural features of the apelin receptor N-terminal tail and first transmembrane segment implicated in ligand binding and receptor trafficking. *Biochim. Biophys. Acta* **2013**, *1828*, 1471−1483.
(39) McCroryjoy, C. A review of methods for the chemical and instrumental analysis of ferrites. *Am. Ceram. Soc. Bull.* **1982**, *61*, 810−816.
(40) Duarte, K.; Justino, C. I. L.; Freitas, A. C.; Duarte, A. C.; Rocha-Santos, T. A. P. Direct-reading methods for analysis of volatile organic compounds and nanoparticles in workplace air. *TrAC, Trends Anal. Chem.* **2014**, *53*, 21−32.
(41) Soo, J. C.; Lee, E. G.; LeBouf, R. F.; Kashon, M. L.; Chisholm, W.; Harper, M. Evaluation of a portable gas chromatograph with photoionization detector under variations of VOC concentration, temperature, and relative humidity. *J. Occup. Environ. Hyg.* **2018**, *15*, 351−360.
(42) Liu, X. Y.; Pawliszyn, J. On-site environmental analysis by membrane extraction with a sorbent interface combined with a portable gas chromatograph system. *Int. J. Environ. Anal. Chem.* **2005**, *85*, 1189−1200.
(43) Aldhafeeri, T.; Tran, M. K.; Vrolyk, R.; Pope, M.; Fowler, M. A review of methane gas detection sensors: recent developments and future perspectives. *Inventions* **2020**, *5*, 28.
(44) Xuecai, X.; Weidong, G.; Chen, L. Analysis study on present situation of emergency rescue in China's coal mines. *Meikuang Anquan* **2017**, *48*, 229−232.
(45) Huan, Y.; Xiaosong, D.; Ming, X.; Chuanwu, Z.; Xiangdong, C. Fast separation on microelectromechanical system-based semi-packed gas chromatography wavy column. *Fenxi Huaxue* **2021**, *49*, 686−692.
(46) Bai, L.; Smuts, J.; Walsh, P.; Qiu, C. L.; McNair, H. M.; Schug, K. A. Pseudo-absolute quantitative analysis using gas chromatography Vacuum ultraviolet spectroscopy - a tutorial. *Anal. Chim. Acta* **2017**, *953*, 10−22.
(47) Giannovario, J. A.; Grob, R. L.; Rulon, P. W. Analysis of trace pollutants in the air by means of cryogenic gas chromatography. *J. Chromatogr. A* **1976**, *121*, 285−294.
(48) Sandoval-Bohorquez, V. S.; Rozo, E. A. V.; Baldovino-Medrano, V. G. A method for the highly accurate quantification of gas streams by on-line chromatography. *J. Chromatogr. A* **2020**, *1626*, No. 461355.
(49) Velasco-Rozo, E. A.; Ballesteros-Rueda, L. M.; Baldovino-Medrano, V. G. A method for the accurate quantification of gas streams by online mass spectrometry. *J. Am. Soc. Mass Spectrom.* **2021**, *32*, 2135−2143.
(50) Ghasemi, J.; Asadpour, S.; Abdolmaleki, A. Prediction of gas chromatography/electron capture detector retention times of chlorinated pesticides, herbicides, and organohalides by multivariate chemometrics methods. *Anal. Chim. Acta* **2007**, *588*, 200−206.
(51) Sfetsas, T.; Michailof, C.; Lappas, A.; Li, Q. Y.; Kneale, B. Qualitative and quantitative analysis of pyrolysis oil by gas chromatography with flame ionization detection and comprehensive two-dimensional gas chromatography with time-of-flight mass spectrometry. *J. Chromatogr. A* **2011**, *1218*, 3317−3325.
(52) Hunter, R. A. Analysis of ethanol in beer using gas chromatography: a side-by-side comparison of calibration methods. *J. Chem. Educ.* **2021**, *98*, 1404−1409.
(53) Lozano, J.; Santos, J. P.; Arroyo, T.; Aznar, M.; Cabellos, J. M.; Gil, M.; Horrillo, M. D. Correlating e-nose responses to wine sensorial descriptors and gas chromatography-mass spectrometry profiles using partial least squares regression analysis. *Sens. Actuators, B.* **2007**, *127*, 267−276.
(54) Xu, X. C.; Huo, X. M.; Qian, X.; Lu, X. Q.; Yu, Q.; Ni, K.; Wang, X. H. Data-driven and coarse-to-fine baseline correction for signals of analytical instruments. *Anal. Chim. Acta* **2021**, *1157*, No. 338386.
(55) Cheng, Z. Z.; Mozammel, T.; Patel, J.; Lee, W. J.; Huang, S. Y.; Lim, S.; Ma, X. B.; Bhargava, S.; Li, C. E. A method for the quantitative analysis of gaseous mixtures by online mass spectrometry. *Int. J. Mass Spectrom.* **2018**, *434*, 23−28.

https://doi.org/10.1021/acsomega.2c02391
ACS Omega 2022, 7, 25443−25457

(56) Wang, C. J.; Rosenfeldt, E.; Li, Y.; Hofmann, R. External standard calibration method to measure the hydroxyl radical scavenging capacity of water samples. *Environ. Sci. Technol.* **2020**, *54*, 1929−1937.
(57) Wang, H.; Fang, K.; Wang, J.; Chang, X. Metabolomic analysis of synovial fluids from rheumatoid arthritis patients using quasi-targeted liquid chromatography-mass spectrometry/mass spectrometry. *Clin. Exp. Rheumatol.* **2021**, *39*, 1307−1315.

https://doi.org/10.1021/acsomega.2c02391
ACS Omega 2022, 7, 25443−25457